A Fast and Sparsity-Aware Generalization of SMART for Tomographic Particle Image Velocimetry

Ioana Barbu and Cédric Herzet
INRIA Rennes - Bretagne Atlantique
Campus de Beaulieu, 35000 Rennes
Email: cedric.herzet@inria.fr

Understanding the tridimensional (3D) motion of turbulent flows is one of the most challenging problems in fluid dynamics. Because the Navier-Stokes equations, describing the spatio-temporal evolution of a fluid, are intractable both at a theoretical and numerical level when dealing with turbulent flows, the idea has soon been proposed to resort to experimental measures. In this line of search, the most common approach is the so-called *"Particle Image Velocimetry"* (PIV) [1] which consists in seeding the fluid with passive particles[1] and accessing to motion measures by processing images of the spatio-temporal evolution of the latter. Recently, researchers have moved their attention to the tridimensional setup, where the 3D motion of a fluid must be inferred from the observation of *a set of images* captured at each time instant. The most-advanced experimental scheme addressing this problem is the so-called *"Tomographic PIV"* system, introduced by Elsinga *et al.* in [2], [3]. The work presented in this paper takes place in this particular applicative context.

We focus hereafter on an intermediate but important step arising in Tomographic PIV: the estimation of the 3D position of the particles from the set of collected images, *i.e.*, the so-called *"Volume reconstruction"* problem [4]. Formally, the task consists in inverting a model of the form

$$\mathbf{y} = \mathbf{D}\mathbf{x} + \text{noise}, \tag{1}$$

where $\mathbf{y} \in \mathbb{R}^m$ is a vector collecting the set of image pixels, $\mathbf{x} \in \mathbb{R}^n$ is a vector such that each element x_j is associated to a possible (discretized) particle position in the volume under study: $x_j = 0$ if and only if there is no particle at the corresponding location; finally, $\mathbf{D} \in \mathbb{R}^{m\times n}$ is a "connection matrix" which relates the collected images to some particle configuration $\mathbf{x}$. We refer the reader to [4, Chapter 2], for a detailed description of the model construction.

Some important facts about model (1): *i)* $m \ll n$ and the inversion of (1) is seriously ill-posed; *ii)* the nonzero elements of $\mathbf{x}$ corresponds to the energy scattered by the particles and are therefore nonnegative, $\mathbf{x} \geq 0$; *iii)* the number of possible positions n is usually much greater than the number of particles in the fluid, that is $\|\mathbf{x}\|_0 \ll n$; *iv)* m and n are typically large (*e.g.*, $m \sim 10^6$, $n \sim 10^9$).

The last item has motivated the TomoPIV community to focus on families of procedures exhibiting low computational and storage requirements. The most popular methodology in the current literature addressing the volume reconstruction problem is undeniably the so-called "Simultaneous Multiplicative Algebraic Reconstruction Technique" (SMART) [5] whose iterates can be expressed as

$$x_j^{(k+1)} = x_j^{(k)} \prod_{i=1}^{m} \left(\frac{y_i}{\mathbf{d}_i^T \mathbf{x}^{(k)}} \right)^{\gamma d_{ij}} \quad \forall\, j, \tag{2}$$

where $\gamma > 0$ and $\mathbf{d}_i \in \mathbb{R}^n$ is the ith row of $\mathbf{D}$. In the sequel, we will use the simple notation $\mathbf{x}^{(k+1)} = \text{SMART}(\mathbf{x}^{(k)})$ to denote the recursion defined in (2).

[1]The particles therefore follow the fluid motion.

SMART suffers from two main drawbacks: *i)* although it implicitly imposes the nonnegativity of the solution, it does not exploit the sparse nature of $\mathbf{x}$; *ii)* it can have a very low speed of convergence, especially for highly-seeded fluids.

In this work, we show that SMART can be simply modified to circumvent these conundrums. We first notice that SMART can be interpreted as a nonlinear projected gradient (NPG) algorithm [6], [7] applied to problem:

$$\min_{\mathbf{x}\in\mathcal{X}} \text{KL}(\mathbf{y}, \mathbf{D}\mathbf{x}), \tag{3}$$

with $\mathcal{X} = \mathbb{R}_+^n$ and where $\text{KL}(\cdot,\cdot)$ denotes the Kullback-Leibler distance between two nonnegative vectors.

With this interpretation in mind, the sparsity of the sought solution can then simply be imposed by adding the additional constraint "$\|\mathbf{x}\|_1 \leq \tau$" to problem (3). This is equivalent to contraining the optimization set to be of the form $\mathcal{X} = \{\mathbf{x} \in \mathbb{R}_+^n | \mathbf{1}^T\mathbf{x} \leq \tau\}$. With this particular choice for $\mathcal{X}$, it can be shown that the NPG iterates still obey a close-form recursion:

$$\mathbf{x}^{(k+1)} = \begin{cases} \tilde{\mathbf{x}}^{(k+1)} & \text{if } \mathbf{1}^T\tilde{\mathbf{x}}^{(k+1)} \leq \tau \\ \tau \frac{\tilde{\mathbf{x}}^{(k+1)}}{\mathbf{1}^T\tilde{\mathbf{x}}^{(k+1)}} & \text{otherwise,} \end{cases} \tag{4}$$

where $\tilde{\mathbf{x}}^{(k+1)} = \text{SMART}(\mathbf{x}^{(k)})$. In words, accounting for the sparsity of $\mathbf{x}$ in the reconstruction process only requires to add a normalization operation to the standard SMART recursion; the normalization occurs as soon as the inequality $\mathbf{1}^T\tilde{\mathbf{x}}^{(k+1)} \leq \tau$ is not satisfied. We will refer to this sparsity-aware version of SMART as "SMARTℓ_1".

The identification of SMART as an instance of NPG algorithm also allows us to propose an accelerated version of this type of procedure. In order to do so, we adopt the strategy proposed in [8, Section 5] which, with a simple modification of the standard NPG updates (inducing no inflation of the complexity order), achieves a rate of decrease of the cost function scaling as $\mathcal{O}(k^{-2})$ (versus $\mathcal{O}(k^{-1})$ for the standard NPG procedure). We will refer to this accelerated version of SMART (resp. SMARTℓ_1) as "A-SMART" (resp. "A-SMARTℓ_1").

Figures 1 and 2 illustrate the performance achieved by the proposed variants of SMART. The abscissa represents the sparsity level of the sought vector $\mathbf{x}$, expressed in terms of the "particles per pixel (ppp) ratio" (see [2]), and the ordinate is the normalized correlation $Q \triangleq \frac{\mathbf{x}^T\mathbf{x}^{(k)}}{\|\mathbf{x}\|\|\mathbf{x}^{(k)}\|}$, a figure of merit commonly used in the Tomographic PIV community. The numerical assessment emphasizes that: *i)* the accelerated version of SMART yields better results in terms of quality of reconstruction, despite solving the same convex problem - this is due to the higher rate of convergence of the latter; *ii)* constraining the sparsity within a noisy setting leads to an improvement of the quality of the estimated vector.

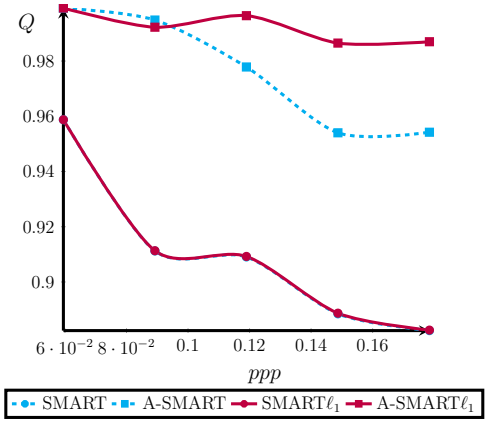

Figure 1. Numerical assessment of the reconstruction quality of $\mathbf{x}^{(100)}$ in an ideal, noise-free scenario for a medium-scale setting (*i.e.*, $m = 6724$, $n = 99944$). The results are averaged on 10 experiments. The relaxation parameter γ is initially chosen as $0.1, 0.05, 0.4$ and 0.8 for SMART, SMARTℓ_1, A-SMART and A-SMARTℓ_1, respectively, and then iteratively adapted following the Armijo rule. We set $\tau = \|\mathbf{x}\|_0$ (where $\mathbf{x}$ is the ground truth whose non-zero coefficients equal 1) in the "sparsity-aware" versions of (A-)SMART. Regardless of the ppp value, which translates here into sparsity levels growing from $\|\mathbf{x}\|_0 = 100$ to $\|\mathbf{x}\|_0 = 300$, SMART algorithms are outperformed by their accelerated versions. We also notice that, while A-SMART is outperformed by its '"sparsity-aware" counterpart, SMART and SMARTℓ_1 superimpose.

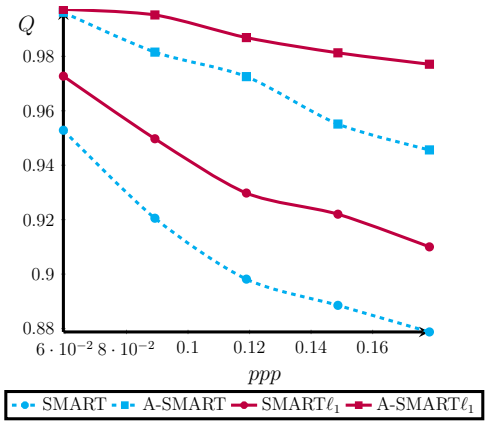

Figure 2. Numerical assessment of the reconstruction quality of $\mathbf{x}^{(100)}$ in a perturbed setting, where y_i is affected by a Gaussian noise of zero mean and standard deviation equal to $0.1y_i$. The other parameters are identical to those used in Fig. 1. The performance of the algorithms follows the pattern observed within a non-perturbed setting (see Fig. 1), with the difference that SMART is outperformed by its '"sparsity-aware" counterpart.

REFERENCES

[1] R.J. Adrian and J. Westerweel, *Particle Image Velocimery*, Cambridge Aerospace Series, 2010.

[2] G. E. Elsinga, *Tomographic particle image velocimetry*, Ph.D. thesis, Technische Universiteit Delft, 2008.

[3] G. E. Elsinga, F. Scarano, B. Wieneke, and B.W. Oudheusden, "Tomographic particle image velocimetry," in *PIV*, 2005.

[4] I. Barbu, *Tridimensional Estimation of Turbulent Fluid Velocity*, Ph.D. thesis, Université Rennes 1, 2014.

[5] C.L. Byrne, "Iterative Image Reconstruction Algorithms Based on Cross-Entropy Minimization," *IEEE Trans. Image Process.*, vol. 2, no. 1, 1993.

[6] A. Beck and M. Teboulle, "Mirror descent and nonlinear projected subgradient methods for convex optimization," *Oper. Res. Lett.*, vol. 31, no. 3, 2003.

[7] S. Petra, C. Schnörr, F. Becker, and F. Lenzen, "B-SMART: Bregman-Based First-Order Algorithms for Non-negative Compressed Sensing Problems," in *SSVM*, 2013.

[8] A. Auslender and M. Teboulle, "Interior gradient and proximal methods for convex and conic optimization," *SIAM J. Sci. Comput.*, vol. 16, no. 3, 2006.

[9] A. Beck and M. Teboulle, "A Fast Iterative Shrinkage-Thresholding Algorithm for Linear Inverse Problems," *SIAM J. Imaging Sci.*, vol. 31, no. 3, 2009.